Journal of Materials Chemistry A

Accepted Manuscript

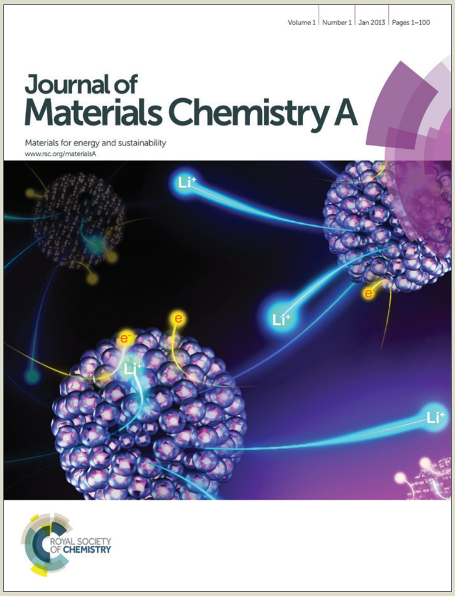

This is an *Accepted Manuscript*, which has been through the Royal Society of Chemistry peer review process and has been accepted for publication.

Accepted Manuscripts are published online shortly after acceptance, before technical editing, formatting and proof reading. Using this free service, authors can make their results available to the community, in citable form, before we publish the edited article. We will replace this *Accepted Manuscript* with the edited and formatted *Advance Article* as soon as it is available.

You can find more information about *Accepted Manuscripts* in the Information for Authors.

Please note that technical editing may introduce minor changes to the text and/or graphics, which may alter content. The journal's standard Terms & Conditions and the Ethical guidelines still apply. In no event shall the Royal Society of Chemistry be held responsible for any errors or omissions in this *Accepted Manuscript* or any consequences arising from the use of any information it contains.

ROYAL SOCIETY
OF **CHEMISTRY**

www.rsc.org/materialsA

Journal of Materials Chemistry A

COMMUNICATION

An integrally skinned asymmetric architecture design for advanced anion exchange membranes in vanadium flow batteries

Received 00th April 20xx,
Accepted 00th April 20xx

DOI: 10.1039/x0xx00000x

www.rsc.org/

Daishuang Zhang,[a] Xiaoming Yan,[b] Gaohong He,*[a] Le Zhang,[a] Xinhong Liu,[a] Fengxiang Zhang,[b] Mengmeng Hu,[a] Yan Dai[a] and Sangshan Peng[a]

A novel integrally skinned asymmetric anion exchange membrane (ISAAEM) with sufficiently low ion exchange capacity (IEC) was proposed to improve the chemical stability of AEM for vanadium flow batteries (VFBs). The ISAAEM with IEC of 0.72 meq g^{-1} showed low area resistance, slight VO^{2+} crossover and good electrochemical performance in VFBs.

Electrical energy storage is essential for integration of renewable energy into the current grid to overcome the variable nature of renewable energy. Among various existing energy storage technologies, vanadium flow battery (VFB) pioneered by M. Skyllas-Kazacos *et al.* at UNSW in 1985,[1] is one of the most promising large-scale energy storage candidates owing to its advantages including flexible design, long life, high efficiency, and capability to withstand fluctuating power input.[2] As a crucial component, an ion-selective membrane separates redox species in the positive compartment and the negative one and at the same time allows the transport of non-reaction ions (such as H^+ and SO_4^{2-}) to maintain electrical neutrality. An ideal membrane is expected to possess low vanadium and water permeation rate, low area resistance (AR), good chemical stability, and low cost.[2c,3] Dupont Nafion® series membranes are most commonly used in VFBs because of high proton conductivity and excellent chemical stability. However, high cost and high vanadium crossover hinder their in-depth commercialization in VFBs.[2c,3] Driven by the demand for cost reduction and vanadium crossover, large amounts of studies focus on developing alternative membranes.[4]

Anion exchange membranes (AEMs) can effectively mitigate the permeation of vanadium ions due to fixed positive charges of AEMs,[5] which can repulse vanadium cations called Donnan exclusion effect. Furthermore, lowering the inclusion of VO_2^+ in the membrane matrix may reduce chemical degradation of the membrane. Based on previously published studies, the chemical stability of AEMs decreases with increasing ion exchange capacity (IEC).[4h] In addition, raising the IEC is accompanied by the increase in vanadium permeability[4k] and water uptake which may result in inevitable swelling, lower mechanical strength, and even disintegration of AEMs.[6] Therefore, it is reasonable to envisage that decreasing the IEC of AEMs as low as possible could serve the purpose of improving chemical durability of AEMs, lowering vanadium permeability and raising mechanical strength. Meanwhile, low IEC (*ca.* 0.7 meq g^{-1} in this work, the threshold value of ~0.65 meq g^{-1}) leads to low ionic conductivity (Fig. S5, ESI†). Similar results were reported.[7] The dense AEMs with low IEC fabricated by the conventional solution casting method usually result in large AR. The AR of AEMs with low IEC can be substantially reduced by decreasing the effective thickness of AEMs. Typically, the thickness of AEMs fabricated by the solution casting method ranges from 30 to 60 μm.[4i,k,6b,8] It is difficult to fabricate much thinner AEMs with a thickness of a few microns which also have poor mechanical strength *via* the conventional solution casting method. Inspired by asymmetric structure comprised of a defect-free thin skin layer supported on a highly porous substructure, as has been commonly applied in membranes for gas separation and pervaporation,[9] we fabricated the ISAAEMs (Fig. 1) with low IEC in the range of 0.72 to 1.01 meq g^{-1} to be employed as the separators of VFBs. This design demonstrated higher stability, lower AR, and better overall electrochemical performance.

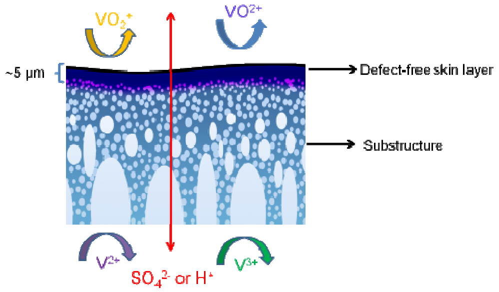

Fig. 1 Schematic cross-section of an integrally skinned asymmetric anion exchange membrane.

---

[a] State Key Laboratory of Fine Chemicals, Research and Development Center of Membrane Science and Technology, School of Chemical Engineering, Dalian University of Technology, Dalian, LN 116024, China. E-mail: hgaohong@dlut.edu.cn; Tel.: +86 411 84986291; Fax: +86 411 84986291.
[b] School of Petroleum and Chemical Engineering, Dalian University of Technology, Panjin, LN 124221, China.

Electronic Supplementary Information (ESI) available: See DOI: 10.1039/x0xx00000x

Journal of Materials Chemistry A Accepted Manuscript

Please do not adjust margins

Journal of Materials Chemistry A Accepted Manuscript

Chloromethylated polysulfone (CMPSf), the selected polymer for membrane formation, was synthesized according to reported method.[10] The degrees of chloromethylation (DCs) of CMPSf were designed to be 40% (denoted as CMPSf-DC40%) and 58% (denoted as CMPSf-DC58%), which were confirmed by ^{1}H NMR (Fig. S1, ESI†). The values for DCs in this work are set lower than DCs values in other studies to circumvent possible chemical degradation incurred by high IEC.[4j,k,5,11] Detailed experimental procedures are described in ESI†. For convenience, the ISAAEMs using CMPSf-DC40% and CMPSf-DC58% as the precursor polymers are denoted as DC40%-20s (IEC = 0.72 meq g^{-1}) and DC58%-20s (IEC = 1.01 meq g^{-1}) (20s is the immersion time in 1-pentanol, shown in ESI†), respectively; the dense QAPSf membrane with IEC of 0.78 meq g^{-1} (see ESI†) that utilizes CMPSf-DC40% as the precursor polymer is abbreviated as Dense DC40%.

The morphology of the as-fabricated ISAAEMs was collected by SEM as shown in Figs. 2a and S2a, b, f and S3a (ESI†). It can be clearly seen (Fig. S2a and b, ESI†) that the ISA morphology, with a defect-free thin skin layer (~5 µm, the magnified cross-sections are shown in Figs. 2a, S2f and S3a, ESI†), was formed, as further confirmed by the CO_2/N_2 separation factor of 28.7 for DC40%-20s (see ESI† for details). The sublayer consisted of a mixture of connected sponge-like pores and macrovoids. The defect-free thin skin layer provides a low hindrance for SO_4^{2-} ions permeation while the porous sublayer provides mechanical strength that benefits cell operations. In contrast, the SEM images of cross-sections of Dense DC40%, fumasep®FAP-450, and Nafion 212 showed homogeneous dense morphologies.

Fig. S6a (ESI†) displays the comparison between AR of the as-made ISAAEMs, homogeneous dense AEMs and commercially available membranes (*i.e.*, Nafion 212 and fumasep®FAP-450). The effective thickness of the DC40%-20s and DC58%-20s membranes was approximately 5 µm (assuming that the AR is directly proportional to the thickness of a membrane), whereas the Dense DC40% thickness was about 30 µm (see Fig. 2b). Compared with Dense DC40% (36.22 Ω cm^2), the AR of DC40%-20s (IEC = 0.72 meq g^{-1}) substantially decreased to 6.72 Ω cm^2 by 81.4%, arising from a substantial decrease in effective membrane thickness (Figs. 2a and S3a), slightly higher than that of Nafion 212 (5.38 Ω cm^2), and concurrently lower than that of fumasep®FAP-450 (9.66 Ω cm^2). This result originates from strong thickness dependence of membrane AR. The DC58%-20s membrane exhibited lower AR (2.88 Ω cm^2) than that of the DC40%-20s membrane, which is due to higher IEC of the DC58%-20s membrane. Fig. S6b shows a linear relationship between the VO^{2+} ion concentrations and diffusion time for each sample, the slope of which reflects the diffusion rate of the VO^{2+} ions. Apparently, the DC58%-20s membrane exhibited the highest VO^{2+} diffusion rate, whereas the Dense DC40% membrane showed the lowest VO^{2+} diffusion rate. In terms of the ability to prevent VO^{2+} ions crossover, the DC40%-20s membrane demonstrated a lower VO^{2+} diffusion rate than those of Nafion 212, fumasep®FAP-450, and the DC58%-20s membrane. The permeability difference between the samples can be ascribed to their different ionic cluster nanostructures (*i.e.*, the size, density and charge nature) and membrane thicknesses. The VO^{2+} permeabilities of the DC40%-20s, DC58%-20s, fumasep®FAP-450, and Nafion 212 membranes were about 0.295×10^{-7}, 2.19×10^{-7}, 4.32×10^{-7}, and 7.54×10^{-7} cm^2 min^{-1}, respectively, as calculated by equation S3 (ESI†). Specifically, the DC40%-20s membrane displayed the minimum VO^{2+} permeability, which may be assigned to the smallest size of ionic clusters and their inherent positive charges (see Fig. S4, ESI†).

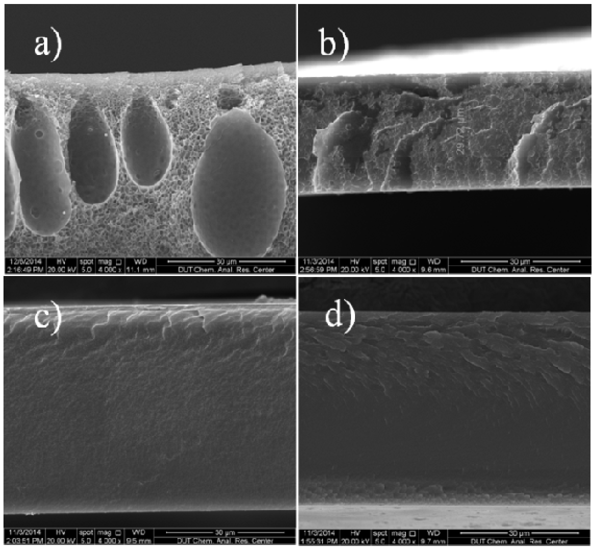

Fig. 2 High-resolution cross-section SEM images of (a) DC40%-20s, (b) Dense DC40%, (c) fumasep®FAP-450, and (d) Nafion 212. All scale bars are 30 µm.

The charge/discharge cycling test using VFB flow cells assembled with various membranes was performed to understand the effect of membrane morphology and IEC on the electrochemical performance of VFB flow cell. The efficiencies of respective flow cells at different current densities ranging from 20 to 100 mA cm^{-2} are shown in Fig. 3. In the case of low IEC (*i.e.*, ~0.72 meq g^{-1}) membrane, the reduction of membrane thickness had little influence on coulombic efficiencies (CEs) when comparing DC40%-20s with Dense DC40%, indicating the vanadium crossover does not increase significantly with the decrease of thickness due to the presence of defect-free skin layer. However, the membrane thickness reduction promoted a significant enhancement in VE. At the same charge/discharge rate, the VE of DC40%-20s reached 82.5%, which was about 16% higher than that of Dense DC40% at 60 mA cm^{-2}. Although the VEs of DC58%-20s were the highest, the VFB assembled with DC58%-20s had the lowest CEs under the entire current density range, in good agreement with the VO^{2+} permeation results (Fig. S6b, ESI†), indicating that high IEC (*i.e.*, 1.01 meq g^{-1}, in this work) if adopted for the membrane of equivalent thickness is not favourable. In addition, the VFB assembled with DC40%-20s had the highest EEs except under current density of 100 mA cm^{-2}, in which case the highest EE was won by Nafion 212 (Fig. 3b). Comparing DC40%-20s with Dense DC40%, as shown in Fig. 3b, the EEs were greatly enhanced by a reduction in effective membrane thickness, coincident with previously reported results.[12] What's more, an increase in membrane IEC led to a drastically falling EEs, originating from the significantly severer vanadium ions crossover (Fig. S6b, ESI†), especially at low current densities.

The cycling test was carried out using a 50 mA cm^{-2} current density at around 30 °C, with a voltage cutoff window ranging from

This journal is © The Royal Society of Chemistry 2015

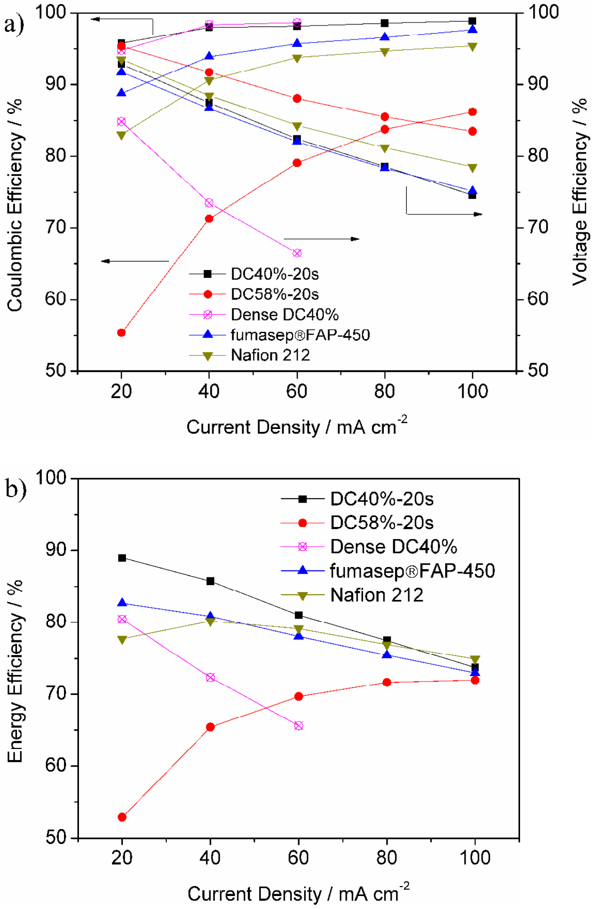

Fig. 3 Electrochemical performance of VFBs employing different membranes as a function of charge/discharge current density. (a) CE and VE; (b) EE. Nafion 212 and fumasep®FAP-450 were used as references. All tests were performed under an identical operating mode.

0.8 to 1.65 V. Capacity decay as a common serious issue for VFB flow cells that employ ion exchange membranes (IEMs) deserves regulation and research attention.[4e,11c,13] The capacity losses per cycle for DC40%-20s, DC58%-20s, Dense DC40%, fumasep®FAP-450, and Nafion 212 were 9.7, 95.1, 1.27, 28.9, and 16.6 mAh/cycle, respectively. The flow cell assembled with DC40%-20s except for Dense DC40% which had inferior EEs and rate capability, exhibited excellent capacity, energy retention capability (Fig. 4 and Figs. S9a, b and d), and slight electrolytes transfer (Table S2, ESI†) over prolonged cycling. Among the various membranes tested, the flow cell with Dense DC40% exhibited the slowest decay in discharge capacity. Unfortunately, it delivered the lowest initial discharge capacity (5.8 Ah L^{-1}, theoretical capacity of 20 Ah L^{-1}) and maintained a low discharge capacity after the first cycle, suggesting a substantially low vanadium utilization ratio, whereas the flow cell with DC40%-20s exhibited an initial discharge capacity of 16.9 Ah L^{-1}, which reached up to 84.5% of theoretical capacity, showing a remarkable improvement compared with 29% of theoretical capacity for the cell equipped with Dense DC40%. As shown in Fig. S9a and b, the effect of the membrane IEC on the cycling performance of VFBs was obtained. It is evident that the discharge

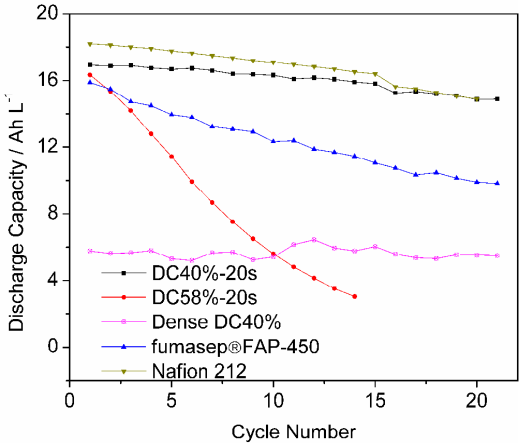

Fig. 4 Electrochemical performance of VFBs employing different membranes over cycling at 50 mA cm^{-2}: discharge capacity over cycling.

capacity fading rate rised significantly with increasing membrane IEC from 0.72 to 1.01 meq g^{-1}. After 14 cycles, the discharge capacities of the VFBs using DC40%-20s and DC58%-20s maintained 94.0% and 18.5% of corresponding initial discharge capacities. It should be noted that the flow battery cycling (assembled with DC58%-20s) had to be terminated owing to severe electrolyte transfer (Table S2, ESI†). Similar trend was also observed with the discharge energy of flow cells (Fig. S9d, ESI†), which determines the ultimate capability of VFB to deliver the useful energy. The discharge energy of the flow cell with DC40%-20s was slightly lower than that of Nafion 212 over the first 20 cycles which derives from lower discharge voltage and capacity of DC40%-20s (Fig. S8a and e, ESI†), whereas the discharge energy of the flow cell with DC40%-20s was apparently higher than those of fumasep®FAP-450, DC58%-20s, and Dense DC40% as separators (see Fig. S9d, ESI†). As shown in Fig. S8c, the VFBs using DC40%-20s, Dense DC40%, fumasep®FAP-450, and Nafion 212, except DC58%-20s, displayed stable cyclic efficiencies over at least 20 cycles (operated for 7 days), thus demonstrating the reliability of these membranes.

In addition, the DC40%-20s membrane with much lower IEC showed a lower swelling ratio, stronger mechanical properties, and better thermal stability than DC58%-20s (Table S1 and Fig. S10, ESI†). The chemical stability of DC40%-20s was much better than that of DC58%-20s, as evidenced by a lower weight loss of DC40%-20s (Table S3, ESI†).

Conclusions

In conclusion, we have designed and demonstrated a novel type of ISAAEM with low IEC and a defect-free thin skin layer for VFBs. Ion exchange membranes with IEC as low as possible (~0.72 meq g^{-1}, in this work) could be applied if ISAAEMs are employed as separators of VFBs. Considering the overtly higher price of functional monomers than that of nonfunctional monomers, less percentage of functional monomers in the IEMs potentially lowers the capital cost of IEMs, which is another favourable factor for promoting the commercialization of IEMs. Compared with conventional dense membrane of identical or similar IEC, the ISAAEM (DC40%-20s)

Journal of Materials Chemistry A Accepted Manuscript

Please do not adjust margins

exhibited dramatically reduced AR. The single cell assembled with it showed excellent electrochemical performances, *i.e.*, higher EE (81.0% *vs.* 65.6%, at 60 mA cm^{-2}) and larger discharge capacity (1539.1 mAh *vs.* 198.2 mAh, at 60 mA cm^{-2}). Furthermore, the single cell with DC40%-20s displayed comparable discharge capacities with the one with Nafion 212 and larger discharge capacities than the ones with fumasep®FAP-450 and DC58%-20s in the prolonged cycling test. The single cell with DC40%-20s exhibited much slower discharge capacity and energy decay rates than those with Nafion 212, fumasep®FAP-450, and DC58%-20s. This work provides new insights into the design, fabrication as well as commercialization of IEMs of VFBs.

Acknowledgements

The authors would like to acknowledge the financial support from the National Science Foundation for Distinguished Young Scholars of China (Grant No. 21125628), the National Natural Science Foundation of China (Grant No. 21406031 and 21476044), the Program for Liaoning Excellent Talents in University (LR2014003), and State Key Laboratory of Fine Chemicals (Panjin) (Grant No. JH2014009) project. We are also grateful to Prof. Huamin Zhang and Prof. Xianfeng Li for providing us with single flow cells.

Notes and references

1 M. Skyllas-Kazacos, M. H. Chakrabarti, S. A. Hajimolana, F. S. Mjalli and M. Saleem, *J. Electrochem. Soc.*, 2011, **158**, R55.

2 (a) W. Wang, Q. Luo, B. Li, X. Wei, L. Li and Z. Yang, *Adv. Funct. Mater.*, 2013, **23**, 970; (b) M. Skyllas-Kazacos, G. Kazacos, G. Poon and H. Verseema, *Int. J. Energy Res.*, 2010, **34**, 182; (c) X. Li, H. Zhang, Z. Mai, H. Zhang and I. Vankelecom, *Energy Environ. Sci.*, 2011, **4**, 1147.

3 B. Schwenzer, J. Zhang, S. Kim, L. Li, J. Liu and Z. Yang, *ChemSusChem*, 2011, **4**, 1388.

4 (a) H. Zhang, H. Zhang, X. Li, Z. Mai and J. Zhang, *Energy Environ. Sci.*, 2011, **4**, 1676; (b) H. Zhang, H. Zhang, X. Li, Z. Mai and W. Wei, *Energy Environ. Sci.*, 2012, **5**, 6299; (c) X. Wei, Z. Nie, Q. Luo, B. Li, B. Chen, K. Simmons, V. Sprenkle and W. Wang, *Adv. Energy Mater.*, 2013, **3**, 1215; (d) W. Wei, H. Zhang, X. Li, H. Zhang, Y. Li and I. Vankelecom, *Phys. Chem. Chem. Phys.*, 2013, **15**, 1766; (e) S. Kim, J. Yan, B. Schwenzer, J. Zhang, L. Li, J. Liu, Z. Yang and M. A. Hickner, *Electrochem. Commun.*, 2010, **12**, 1650; (f) C. Fujimoto, S. Kim, R. Stains, X. Wei, L. Li and Z. G. Yang, *Electrochem. Commun.*, 2012, **20**, 48; (g) D. Chen, S. Wang, M. Xiao and Y. Meng, *Energy Environ. Sci.*, 2010, **3**, 622; (h) S. Zhang, C. Yin, D. Xing, D. Yang and X. Jian, *J. Membr. Sci.*, 2010, **363**, 243; (i) D. Chen, M. A. Hickner, E. Agar and E. C. Kumbur, *Electrochem. Commun.*, 2013, **26**, 37; (j) H. Zhang, H. Zhang, F. Zhang, X. Li, Y. Li and I. Vankelecom, *Energy Environ. Sci.*, 2013, **6**, 776; (k) Z. Mai, H. Zhang, H. Zhang, W. Xu, W. Wei, H. Na and X. Li, *ChemSusChem*, 2013, **6**, 328; (l) J. Ma, Y. Wang, J. Peng, J. Qiu, L. Xu, J. Li and M. Zhai, *J. Membr. Sci.*, 2012, **419-420**, 1; (m) Z. Yuan, X. Li, Y. Duan, Y. Zhao and H. Zhang, *Polym. Chem.*, 2015, DOI: 10.1039/C5PY00482A.

5 (a) M.-s. J. Jung, J. Parrondo, C. G. Arges and V. Ramani, *J. Mater. Chem. A*, 2013, **1**, 10458; (b) W. Xu, Y. Zhao, Z. Yuan, X. Li, H. Zhang and I. Vankelecom, *Adv. Funct. Mater.*, 2015, **25**, 2583.

6 (a) J. R. Varcoe, P. Atanassov, D. R. Dekel, A. M. Herring, M. A. Hickner, P. A. Kohl, A. R. Kucernak, W. E. Mustain, K. Nijmeijer, K. Scott, T. Xu and L. Zhuang, *Energy Environ. Sci.*, 2014, **7**, 3135; (b) M. Tanaka, K. Fukasawa, E. Nishino, S. Yamaguchi, K. Yamada, H. Tanaka, B. Bae, K. Miyatake and M. Watanabe, *J. Am. Chem. Soc.*, 2011, **133**, 10646; (c) N. Li, L. Wang and M. Hickner, *Chem. Commun.*, 2014, **50**, 4092.

7 (a) E. Moukheiber, G. De Moor, L. Flandin and C. Bas, *J. Membr. Sci.*, 2012, **389**, 294; (b) Y. A. Elabd, C. W. Walker and F. L. Beyer, *J. Membr. Sci.*, 2004, **231**, 181.

8 Q. Li, L. Liu, Q. Miao, B. Jin and R. Bai, *Chem. Commun.*, 2014, **50**, 2791.

9 (a) M. H. V. Mulder, J. O. Hendrikman, J. G. Wijmans and C. A. Smolders, *J. Appl. Polym. Sci.*, 1985, **30**, 2805; (b) J. Kurdi and A. Y. Tremblay, *J. Appl. Polym. Sci.,* 1999, **73**, 1471; (c) M. R. Kosuri and W. J. Koros, *J. Membr. Sci.*, 2008, **320**, 65.

10 X. Yan, G. He, S. Gu, X. Wu, L. Du and Y. Wang, *Int. J. Hydrogen Energy*, 2012, **37**, 5216.

11 (a) S. Gu, R. Cai, T. Luo, Z. Chen, M. Sun, Y. Liu, G. He and Y. Yan, *Angew. Chem.*, Int. Ed., 2009, **48**, 6499; (b) S. Gu, R. Cai and Y. Yan, *Chem. Commun.*, 2011, **47**, 2856; (c) D. Chen, M. A. Hickner, E. Agar and E. C. Kumbur, *ACS Appl. Mater. Interfaces*, 2013, **5**, 7559.

12 (a) D. Chen, M. A. Hickner, E. Agar and E. C. Kumbur, *J. Membr. Sci.*, 2013, **437**, 108; (b) Y. Li, X. Li, J. Cao, W. X and H. Zhang, *Chem. Commun.*, 2014, **50**, 4596.

13 (a) Q. Luo, L. Li, W. Wang, Z. Nie, X. Wei, B. Li, B. Chen, Z. Yang and V. Sprenkle, *ChemSusChem*, 2013, **6**, 268; (b) C. Ding, H. Zhang, X. Li, H. Zhang, C. Yao and D. Shi, *ChemSusChem*, 2013, **6**, 1262.

Journal of Materials Chemistry A Accepted Manuscript

This journal is © The Royal Society of Chemistry 2015